NASA Technical Memorandum 79059

(NASA-TM-79059) EFFECT OF FORWARD VELOCITY AND CROSSWIND ON THE REVERSE-THRUST PERFORMANCE OF A VARIABLE-PITCH FAN ENGINE (NASA) 21 p HC A02/MF A01 CSCL 21E G3/07

N79-15049

Unclas 42892

EFFECT OF FORWARD VELOCITY AND CROSSWIND ON THE REVERSE-THRUST PERFORMANCE OF A VARIABLE-PITCH FAN ENGINE

D. C. Reemsnyder and D. A. Sagerser
Lewis Research Center
Cleveland, Ohio

TECHNICAL PAPER to be presented at the Seventeenth Aerospace Sciences Meeting sponsored by the American Institute of Aeronautics and Astronautics
New Orleans, Louisiana, January 15-17, 1979

EFFECT OF FORWARD VELOCITY AND CROSSWIND ON THE REVERSE-THRUST PERFORMANCE OF A VARIABLE-PITCH FAN ENGINE

D. C. Reemsnyder and D. A. Sagerser
National Aeronautics and Space Administration
Lewis Research Center
Cleveland, Ohio

Abstract

A full-size variable-pitch fan engine was tested in the Ames 40- by 80-foot wind tunnel to determine the effect of forward velocity and crosswind on reverse-thrust performance. Two flight-type inlet configurations were tested, and a flared fan nozzle was installed as an inlet for reverse-thrust operation. Steady-state reverse-thrust performance was obtained up to 54 m/s (105 knots). An abrupt decrease in reverse thrust occurred at about 30 m/s (60 knots). Reverse thrust was established following forward-to-reverse thrust transients both statically and with forward velocities only up to 30 m/s.

Summary

The variable-pitch, Q-Fan T-55 engine was tested for reverse-thrust performance in the NASA Ames 40- by 80-foot wind tunnel at forward velocities up to 54 m/s (105 knots) and at angles of attack up to 22°. The engine had a fan nozzle flared outward for reverse-thrust operation (exlet), and was tested with two flight-type inlets, differing primarily in inlet throat diameter.

During the wind-tunnel tests with forward velocity, an unexpected transition from full to partial reverse thrust occurred abruptly as the tunnel velocity was increased to about 30 m/s (60 knots) with the engine power setting held constant. The partial reverse-thrust mode was characterized by significantly lower reverse thrust, a higher fan operating line, lower inlet lip and exlet static pressures, and negligible fan jet penetration into the free stream as compared with the full reverse-thrust mode. The primary cause of the decreased reverse thrust in the partial mode appears to be the significant changes in the pressure forces on the nacelle as forward velocity increased. Considerable hysteresis was associated with reverting to the full reverse-thrust mode by decreasing tunnel velocity.

Steady-state reverse thrust increased, as expected, with increasing tunnel velocity in the full reverse-thrust mode. In the partial reverse-thrust mode, increasing forward velocity resulted in a gradual decrease in engine reverse thrust. The fan operating line moved higher with increasing forward velocity in the partial reverse-thrust mode, whereas it moved lower in the full reverse-thrust mode.

Limited crosswind tests showed that in some cases variations in angle of attack caused the engine to change reverse-thrust modes (partial to full and full to partial). Buffetting and high engine vibrations occurred at angles of attack above 20°.

In the forward-to-reverse thrust transient tests, the "overshoot" blade angle technique proved effective in reducing the time required to establish reverse thrust with a flight-type inlet both statically and with forward velocity. For these transients the engine control computer moved the fan blade angle beyond the final reverse blade angle, held it at the overshoot blade angle for a short time, and then returned it to the final reverse fan blade angle. Forward-to-reverse thrust transients were accomplished only up to a forward velocity of 30 m/s (60 knots) with the low-Mach inlet and up to 20 m/s (40 knots) with the high Mach inlet. Forward velocity requires the overshoot blade angle to be increased to establish and maintain reverse thrust. The high-Mach inlet requires a higher overshoot blade angle to establish reverse thrust than the low-Mach inlet under similar operating conditions.

In view of the abrupt transition to a partial-reverse-thrust mode and the low, 30-m/s limit for successful forward-to-reverse thrust transients, it is apparent that advanced variable-pitch turbofan engines require additional development to provide adequate, reproducible reverse-thrust levels for successful deceleration of aircraft.

Introduction

Variable-pitch-fan engines may be attractive for future short-haul aircraft if sufficient reverse thrust is available for aircraft deceleration after touchdown. Thrust reversal is obtained in these engines by changing fan blade pitch about 90°, which causes the fan airflow to enter the fan duct nozzle and exhaust through the fan inlet. This capability would eliminate the heavy and costly thrust reverser systems required for current fixed-pitch turbofan engines. The NASA Lewis Research Center has supported the development of advanced technology for a quiet, clean, high-bypass-ratio turbofan engine for future short-haul aircraft. A major portion of this effort is the Quiet, Clean, Short-Haul Experimental Engine (QCSEE) Program.[1] A summary of previous work related to reverse-thrust operation of variable-pitch fan engines is discussed in reference 2.

As part of the program to develop the propulsion-system technology for short-haul aircraft, NASA has also supported testing of Hamilton Standard's Q-Fan T-55 engine. This engine features a full-size, dynamically controllable, variable-pitch fan. Previous tests,[3-6] conducted on outdoor static-test rigs, have investigated steady-state, reverse-thrust performance and dynamic performance during forward-to-reverse thrust transients. During the tests of reference 6, no difficulty was experienced in establishing reverse thrust with a bellmouth inlet for either engine startups with the fan blades in a fixed reverse-thrust position or for forward-to-reverse thrust transient tests. However, with a flight-type inlet (smaller outlet area in reverse thrust), it was more difficult to establish reverse thrust both for startups and for transients. Some difficulty in establishing reverse thrust during startup was also observed during reverse-thrust tests of a model of the QCSEE fan with a flight-type inlet.[7] At some reverse-thrust blade

NASA TM-79059
AIAA 79-0105

angles the fan would initially be in a stalled condition at startup. Then, as speed was increased stall would clear and reverse thrust would be generated. The speed at which stall cleared was found to be a function of the preset reverse-fan blade angle.

In both the Q-Fan T-55 engine tests and the QCSEE fan model tests, increasing the reverse fan blade angle (towards flat pitch) helped the fan to clear stall and establish reverse thrust. The full benefit of increased fan blade angle could not be demonstrated during the tests of the Q-Fan T-55 engine because of the limited blade travel in the pitch-change actuator system. The actuator was therefore modified to allow for operation at higher reverse fan blade angles for the wind-tunnel tests reported herein.

Low-speed wind-tunnel tests were conducted at NASA Lewis with a 50.8-cm (20-in.), 1.15-pressure-ratio, adjustable-pitch fan simulator.[8] Measured steady-state reverse thrust decreased gradually with increasing tunnel velocity to about 50 percent of static reverse thrust at a typical short-haul landing speed of 41 m/s (80 knots). No apparent increase in reverse thrust was observed with increasing tunnel velocity, as might be expected due to the ram drag.

To increase the technical knowledge of variable-pitch fans, an investigation into the effect of forward velocity and crosswind on reverse-thrust performance of the Q-Fan T-55 engine was conducted in the NASA Ames 40- by 80-foot wind tunnel. NASA Lewis directed the test program; NASA Ames operated the wind tunnel and force balance and provided hardware and test support; Hamilton-Standard (prime contractor - NAS3-20038) supplied and operated the test engine; and the Boeing Company, under subcontract to Hamilton-Standard, was responsible for data acquisition and reduction.

The test objectives of the program reported herein were to determine the effect of forward velocity and angle of attack on steady-state reverse-thrust performance, to determine the effect of forward velocity on forward-to-reverse thrust transient performance, and to determine the effectiveness of an overshoot blade angle technique to establish reverse thrust during a transient. Tunnel velocities during the tests were set from 0 to 54 m/s (105 knots). The model angle of attack was varied from 0° to 22°. The maximum fan speed was 3255 rpm (97.5 percent $N/\sqrt{\theta}$). And the fan blade angle range was 43° (forward) to 168° (reverse through feather pitch).

Apparatus and Procedure

Test Facility

The NASA Ames wind tunnel has a closed, 12.2- by 24.4-m (40- by 80-ft) test section with semicircular sides of 6.1 m (20 ft) radii, and a closed-circuit air return passage. Air is driven in the wind tunnel by six 12.2-m (40-ft) diameter fans, which are powered by six 4474-kW (6000-hp) electric motors. The tunnel operates with a stagnation pressure equal to atmospheric. Stagnation temperature varies from ambient upwards, due to heat from the entrained products of combustion and the tunnel drive system.

A photograph of the engine installed in the wind tunnel is shown in Fig. 1. The engine with nacelle was mounted on a single, hollow-column pylon approximately 3.8 m (150 in.) from the wind-tunnel floor. The pylon, in turn, was attached to the facility's floor-mounted semispan model turntable located on the wind tunnel's vertical centerline. The semispan turntable, strut, and nacelle were "on balance" for measuring model forces. A large fairing or "wind shield," off balance, protected the turntable and strut surfaces from the wind-tunnel aerodynamic forces. The nacelle was yawed in the horizontal plane by means of the tunnel turntable to simulate operation at the various inlet angles of attack. The inlet top to bottom (0° to 180°) axis was located on the horizontal plane of the wind tunnel. White tufts were installed on a wire on the engine horizontal centerline about 3.0 m (10 ft) in front of the engine inlet highlight and on the external surface of the low-Mach inlet nacelle (Fig. 1).

Engine Test Configuration

The test model consisted of an inlet, a variable-pitch fan, a gas-turbine core engine, an exlet (reverse flow inlet), and appropriate fairings, nozzles, etc. The Hamilton-Standard Q-Fan demonstrator is a 1.397-m (55-in.), 13-bladed, variable-pitch fan with a Lycoming T-55-L-11A, 2796-kW (3750-hp) gas-turbine core engine. A schematic of the Q-Fan T-55 engine showing the major components and the instrumentation station designations is shown in Fig. 2 with the low-Mach inlet and exlet in place. The engine has a 17:1 bypass ratio and is driven through a 4.75:1 gear reduction to a maximum speed of 3365 rpm. The fan has a 0.645-m (25.4-in.) diameter, semielliptical nose dome fairing. The fan exit nozzle was an annulus with an exit area of 1.064 m^2 (1649 in^2). The reverse-thrust exlet with a 30° (half angle) conical flare was mounted on the aft end of the fan exit nozzle for reverse-thrust operation. The core engine exit nozzle supplied with the engine had an exit area of 0.254 m^2 (394 in^2). The core engine had no centerbody, and core tailpipe was about 12.7 cm (5 in.) shorter than it was in previous configurations.

The variable-pitch actuator was modified with a new blade trunnion to increase the maximum reverse-fan blade angle by about 8° to allow for a greater overshoot blade angle. A schematic of the variable-pitch fan blade in the forward and the reverse-through-feather pitch configurations is shown in Fig. 3 with the blade-angle convention noted. In the reverse-through-feather configuration the blade camber correctly turns the flow toward axial, but the leading and trailing edges are reversed.

Two flight-type inlets were tested with the Q-Fan T-55 engine, and a comparison of their characteristics is presented in Table 1. The Boeing Lift/Cruise low-Mach inlet had an asymmetric inlet contour with the windward side having a higher contraction ratio (1.76) than the leeward side (1.30). At a given inlet station both the internal and external contours are of circular cross section with offset centers. The high-Mach inlet was geometrically similar to the QCSEE inlet, which was designed with a high throat Mach number (0.79) for fan inlet noise suppression. Because of the smaller inlet throat diameter, the high-Mach inlet has a ratio of inlet throat to fan face flow area of 0.81, as

compared with 0.93 for the low-Mach inlet.

Instrumentation - Reverse-thrust Configuration

Steady-state reverse-thrust instrumentation (Fig. 2) included two 10-element total-pressure rakes in the aft fan duct (station 1) and 2 at the fan face (station 2); eight 6-element total-pressure rakes at the compressor face (station 2.5); 3 total-temperature probes in aft fan duct and 1 at the compressor face; and 7 static-pressure taps in the aft fan duct, 11 on the exlet, 45 on the low-Mach inlet (22 on the high Mach inlet), and 8 at the compressor face. Fan face rakes are set at 45° with respect to engine centerline. Circumferential locations of the rakes are also shown in Fig. 2.

Wind tunnel instrumentation measured tunnel total pressure, dynamic pressure, and total temperature. In addition, the model lift, drag and side forces, and pitch, yaw, and rolling moments were measured by the balance system. For most transient tests the force balance was locked to protect the sensitive balance knife edges and mechanism.

Engine operational instrumentation included fan blade angle, power lever angle, compressor speed, turbine speed, turbine interstage temperature, engine torque, vibration, and dynamic pressure transducers. Five strain gauges installed on selected fan blades were monitored and recorded on magnetic tape to insure operation of the fan blades within their structural design envelope.

For the forward-to-reverse transient tests, data were recorded on magnetic tape and displayed on an oscillograph. All fan rakes were removed for the transient tests.

Data Reduction

Various test parameters were recorded on several data systems: engine performance data on a Boeing steady-state data acquisition system, wind tunnel and force information on the facility data system, fan operation and health on a Hamilton Standard tape recording system, and selected parameters for transient tests on a Boeing tape recording system. Engine operational parameters were also recorded on the engine logs.

Steady-state reverse-thrust data reduction included the calculation of the following parameters: (1) corrected tunnel and force balance parameters, (2) measured corrected engine reverse thrust along engine centerline, (3) fan speed, (4) fan average total- and static-pressure ratios, (5) aft fan duct airflow, (6) exlet (fan duct) total-pressure recovery and distortion, (7) core engine speed, torque, and power, and (8) core compressor airflow, total and static pressures, distortion, and total-pressure recovery.

Forward-to-reverse thrust transient data reduction at NASA Lewis consisted of digitizing the analog data from the magnetic tapes, converting to engineering units, performing calculations, and presenting the data in both tabular and graphical form. The digitized data were averaged (about 30 data points per average) to produce a data point for each 0.01 s from the start to end of the transient. Steady-state initial and end conditions are determined from a 2.0-s average of data before and after the actual transient. Calculated parameters throughout the transient include fan blade-angle position and rate, corrected fan and core speeds, corrected core engine torque and power, fan static-pressure ratios and differences, fan blade stresses, and dynamic pressure fluctuations. Calculated values for each successful transient include actual overshoot blade angle, dwell time, total thrust response time, actual blade travel time, flow reattachment time, and the thrust delay time after flow reattachment (see the appendix for definition of terms). Maximum values of engine torque, fan blade stress, and fan blade pitch change rate are recorded.

Test Procedure

For the steady-state reverse-thrust tests all engine startups were accomplished with a preset reverse fan blade angle under static (tunnel off) conditions. The engine was accelerated to idle and checked for reverse thrust and flow by observing the force-balance (thrust) reading and the external tufts. If negligible reverse thrust was observed, speed and/or fan blade angle β was increased until reverse thrust and flow was initiated.

To define the effect of forward velocity, the engine was set at a fixed operating condition (β and speed), and the tunnel velocity was increased to the desired level. Steady-state reverse-thrust performance data were obtained. Then, either engine operating conditions were changed at constant tunnel velocity, or tunnel velocity was changed at constant engine operating conditions. The engine angle of attack was varied at constant engine operating conditions and constant tunnel velocity.

Steady-state forward-thrust performance data were obtained with the reverse exlet to define the initial steady-state forward operating condition for the forward-to-reverse thrust transients. Engine operating conditions were established for both approach and takeoff at static conditions and at a tunnel velocity of 40 m/s (80 knots).

For the forward-to-reverse transients the engine was set at constant forward-thrust operating conditions and constant tunnel velocity. Inputs for each transient were programmed into the engine control computer, for example, thrust setting lever, power-lever angle, fan-blade pitch-change rate, number of degrees of overshoot beyond the final reverse blade angle, and dwell time at the overshoot blade angle. All forward-to-reverse thrust transients were initiated from either an approach or takeoff engine power setting. All transients had the same programmed reverse-thrust end condition with a fan blade angle of 148° at 85 percent of corrected fan speed. During static (tunnel off) running, the engine in the forward-thrust mode pumps the tunnel and induces a forward velocity up to about 10 m/s at the initiation of the transient.

Steady-State Reverse-Thrust Peformance

Reverse-thrust performance was obtained with the engine and the wind tunnel at steady-state operating conditions. Operational boundary conditions were determined with relatively slow changes in either fan blade angle or fan speed.

Reverse-Thrust Starting and Stall-Unstall Characteristics at Static Conditions

To better understand the starting and stall-unstall characteristics of this fan, a number of manually controlled variations in fan speed and fan blade angle were conducted to determine the conditions where reverse thrust was established or lost. These quasi steady-state results, which can also be obtained in model fan tests, may be correlated with forward-to-reverse thrust transient performance.

All engine startups for reverse-thrust performance were attempted with a preset reverse fan blade angle under static (tunnel off) conditions: eight with the low-Mach inlet and three with the high-Mach inlet. Results of these tests are shown in Fig. 4. With the low-Mach inlet and a fan blade angle of 150°, reverse thrust was observed at the lowest stabilized fan speed. With low fan blade angles from 147° to 149.5°, the fan was stalled initially, and fan speed had to be increased to clear stall and establish reverse thrust. An abrupt transition occurred from the fully stalled, negligible reverse-thrust mode to the unstalled reverse-thrust mode. Considerable hysteresis was also observed in that once reverse thrust was established, no transitions were observed back to the fully stalled mode by decreasing fan speed. At a fan blade angle of 146° reverse thrust could not be established even up to 81 percent fan speed. The high-Mach inlet had similar characteristics, but the smaller effective outlet throat area in reverse made it more difficult to establish reverse thrust. Unstalling of the fan by increasing fan speed at some reverse fan blade angles and not returning to a stalled condition when decreasing fan speed was also observed during reverse-thrust tests of a model of the QCSEE variable pitch fan.[7]

In the above cases where the fan remained stalled during startup, reverse thrust could be established by increasing fan blade angle at a constant fan speed. A typical example of the reverse-thrust hysteresis with fan blade angle is presented in Fig. 5(a) at 75 percent of fan speed with the low-Mach inlet. Negligible reverse thrust was observed initially as β was increased from 142° to 149°. At β = 149°, the engine abruptly changed to the full reverse-thrust mode. Reverse thrust increased as β was then decreased to 136°, where core speed and turbine temperature limits were encountered. Once reverse thrust was established at 149°, the fan blade angle could be varied considerably (±10° to ±15°) without the engine reverting to the fully stalled mode, indicating a large hysteresis in performance with fan blade angle. It should be noted that the desired blade angle operating range is below 149° to obtain high reverse thrust. But operation at these low blade angles may be impossible without first establishing reverse thrust at higher fan blade angles. Reverse-thrust testing of a variable-pitch fan and inlet combination may therefore require a means of adjusting β during fan operation to obtain high values of reverse thrust.

The transition blade angle at other fan speeds is presented in Fig. 5(b) for both the low- and high-Mach inlets. For the low-Mach inlet a β of 148° or more is required to establish reverse thrust by increasing β at constant fan speed, whereas the high-Mach inlet requires 156° or above. As β was decreased, either a core limit or fan stall was encountered. For the low-Mach inlet at 50 percent of fan speed, once reverse thrust was established, satisfactory operation was experienced until a β of 133° was reached, where the fan approached stall. Above 50 percent fan speed a core limit was reached before the fan stalled as β was reduced.

Reverse-Thrust Performance at Static Conditions

Steady-state reverse-thrust performance at static conditions (tunnel off) is presented in Fig. 6 at various reverse-fan blade angles and fan speeds. To obtain these data, reverse thrust was initially established by either increasing fan speed or fan blade angle, as was previously discussed. Performance obtained with the low-Mach inlet is presented in Fig. 6(a) and that with the high-Mach inlet in Fig. 6(b). The effect of inlet configuration on reverse thrust is very slight. Performance trends at static conditions are similar to those obtained in previous tests of this engine (ref. 3). Reverse thrust increases with increasing fan speeds and with decreasing reverse-fan blade angles down to 136°. At the lower fan blade angles, high fan speeds could not be obtained because of core speed and turbine temperature limits, as noted in the figure.

Effect of Forward Velocity on Reverse-Thrust Performance

Previous steady-state reverse-thrust testing of the Q-Fan T-55 engine in outdoor static-test stands showed that the engine could operate in one of two modes: a full reverse-thrust mode and a negligible reverse-thrust, stalled-fan mode. During the wind-tunnel tests with forward velocity, a third, partial reverse-thrust mode was observed. The partial reverse-thrust mode was characterized by lower reverse thrust and negligible fan jet penetration into the free stream than the full reverse-thrust mode. During the wind-tunnel tests the engine would abruptly change from the full reverse-thrust mode to the partial reverse-thrust mode as the tunnel velocity was increased at constant engine power setting. Once the engine shifted from the full to the partial reverse-thrust mode, considerable hysteresis was associated with reverting to the full reverse-thrust mode. As subsequent figures will show, the fan remained stable and did not stall during the transition from full to partial reverse thrust, but significant changes in static pressures (and forces) on the inlet and exlet occurred. This indicates that a change in flow over the nacelle is probably the primary cause of the reduction in reverse thrust during the transition.

The effect of increasing forward velocity on reverse-thrust performance with the engine set at a fixed fan blade angle and fan speed is presented in Fig. 7 for the low Mach inlet. Generally, it can be seen that as tunnel velocity increases reverse thrust increases until a point where the engine abruptly changes to a partial reverse-thrust mode. This transition appears to be a function of fan speed, as noted in the figure. The transition to the partial reverse-thrust mode occurred at about 30 m/s and resulted in a significant (∿30 percent) decrease in reverse thrust, a slight (∿5 percent) decrease in fan speed, and negligible fan jet penetration to the tufts. Fan speed was readjusted to the initial value by increasing the engine power

setting and the tests were continued at constant N and β. The engine operated satisfactorily in the partial reverse-thrust mode with a gradual decrease in reverse thrust to a forward velocity of 54 m/s. In the wind-tunnel tests of a 50.8-cm fan model,[8] reverse thrust decreased gradually with increasing tunnel velocity from static up to 43 m/s. No abrupt transition was noted.

The engine with the high-Mach inlet (smaller effective outlet throat area in reverse) behaved similarly to the low-Mach inlet as forward velocity was varied. The transition from full to partial reverse thrust occurred abruptly at about a forward velocity of 30 m/s at high fan speeds, and was similarly characterized by decreased reverse thrust, decreased fan speed, and negligible fan jet penetration to the tufts.

A typical reverse-thrust hysteresis loop with tunnel velocity is shown in Fig. 8 for a β of 148° at 85 percent of fan speed. It should be noted that, once the engine transitioned to the partial reverse-thrust mode, tunnel velocity could be reduced to less than 20 m/s (below the transition zone) without reverting back to the full reverse-thrust mode. Data points designated A, B, and C will be compared and discussed in the next section.

Analysis of Forward Velocity Effects

To help understand the effect of forward velocity and the transition from the full to the partial reverse-thrust mode, several more detailed performance characteristics will be examined: exlet and core inlet total-pressure recovery, fan stage performance, inlet and exlet surface static pressures, and visual flow observations. Comparisons will be made of these characteristics at conditions A, B, and C (Fig. 8), where point A is the static condition, point B is full reverse thrust at 20 m/s, and point C is partial reverse thrust at 20 m/s. Points A, B, and C are all at a β of 148° and a fan speed of 85 percent.

First exlet and core compressor-face total-pressure recovery will be examined. As noted in Fig. 9, exlet total-pressure recovery decreases from about 0.995 to about 0.975, while the compressor-face recovery decreases from about 0.900 to about 0.885 in going from static to 54 m/s. No changes in the exlet or core total-pressure recovery are apparent in Fig. 9 that would account for the transition from the full to the partial reverse-thrust mode (from point B to C). The effect of tunnel velocity on the 30° conical exlet total-pressure recovery is similar to that obtained in Refs. 9 and 10 with a 14-cm (5.5 in.) diameter exlet model.

The fan performance map for the steady-state reverse-thrust tests is presented in Fig. 10 for β = 148° at various tunnel velocities. The static (tunnel off) fan operating line is shown for reference. A slightly lower than static fan operating line (OL) was observed at a forward velocity of 20 m/s in the full reverse-thrust mode. Measured fan rotor flow increased about 5 percent at constant fan speed. A significantly higher fan operating line is observed at 20 m/s in the partial reverse-thrust mode as compared with the full reverse-thrust mode. This shift in fan OL correlates with the sudden change in reverse thrust from the full to the partial reverse-thrust modes. However, the decrease in ideal fan reverse thrust (based on fan flow and fan outlet pressure) from point B to C is significantly less than the measured change in thrust. In the partial reverse-thrust mode increasing forward velocity up to 54 m/s caused the fan OL to move even higher, indicating evidence of a back pressure effect on the fan due to the increased forward velocity. The fan static-pressure ratio in reverse was examined and correlates well with the fan total-pressure ratio, suggesting that the measured fan OL shift is not due to measurement errors caused by the fixed location of the fan outlet total total-pressure rakes at the fan face.

Next, a series of pressure profiles affecting fan operation and reverse thrust are presented in Figs. 11 to 14 for conditions A, B, and C to further examine the effect of forward velocity and the transition from full to partial reverse thrust. The profiles are presented in the order that the flow passes through the engine in reverse thrust: exlet, aft fan duct, fan face, and inlet.

Since pressure forces on the flared exlet can be very large and directly affect the net reverse thrust, the axial static pressure distribution along the exlet internal surface is shown in Fig. 11(a). The location of static-pressure taps is indicated on the exlet (e) in Fig. 2. In the full reverse-thrust mode at 20 m/s (condition B), static pressures were signficiantly lower than those measured at static conditions (A), indicating a large increase in the exlet's contribution to reverse thrust. The transition from the full to partial reverse-thrust mode at 20 m/s (condition B to C) is characterized by a significant increase in the exlet static pressure, indicating a large decrease in the exlet's reverse-thrust contribution. This change in pressure was also evident when full and partial reverse-thrust mode points were compared at equal flow rates, which comparison suggests that a change occurred in the engine external flow field. Because no static pressures were measured on the external surface, the net change in exlet force cannot be accurately determined. However, the variations in the exlet pressure forces correlate very well with the variations in measured reverse thrust at the three conditions compared.

To evaluate exlet total-pressure recovery and the fan inlet pressure in reverse, radial total-pressure profiles in the aft fan duct are compared for the three conditions in Fig. 11(b). Both the full and partial modes at 20 m/s showed slightly lower pressures than at the static condition, but all three profiles were similar. Exlet total-pressure recovery (P_{T1}/P_{T0}) is based on this aft fan-duct radial profile.

The fan-outlet total-pressure in reverse is defined by the radial total-pressure profiles at the fan face. (See Fig. 12.) As was the case in the aft fan duct, the fan outlet profiles are similar for conditions A, B, and C. Below ambient pressures in the fan-hub region are a result of high swirl secondary flows. The difference in fan-outlet absolute pressure from condition A to B reflects the decrease in exlet total-pressure recovery with forward velocity, and from condition B to C the significant increase in fan pressure ratio. The similarity of fan-inlet and -outlet radial pressure profiles for conditions A, B, and C indicates that the change in the fan operating line was apparently due to the flow changes external to the fan.

One indication of such a change is shown in Fig. 13, where the axial static-pressure distribution in the asymmetric low-Mach inlet is presented for the windward thick-lip side of the inlet. Similar characteristics were observed on the thin-lip side of the inlet. At 20 m/s in the full reverse-thrust mode (condition B), the inlet surface static-pressure profile differs only slightly from that obtained at static conditions (condition A). However, in the partial reverse-thrust mode at the same forward velocity (condition C), the location of the minimum static pressure moved significantly forward of the throat, and the level of static pressures increased significantly between the minimum pressure and the fan face. The significantly higher static pressure at the inlet throat results in the higher fan operating line.

Since inlet lip pressure forces can be very large and directly affect the net reverse thrust, the inlet static pressure data from Fig. 13 is plotted versus inlet lip projected area in Fig. 14 for the windward, thick-lip side of the low-Mach inlet. Similar characteristics were observed on the thin-lip side of the inlet. Again, inlet radial profiles are very similar at static conditions, and at 20 m/s in the full reverse-thrust mode. In the partial reverse-thrust mode at 20 m/s, the inlet radial profile shifted considerably, resulting in significantly lower lip static pressures, which have a decreasing effect on reverse thrust. The location of the minimum static pressure moved significantly outward radially, which suggests that the flow is tending to follow the lip contour radially outward rather than separate near the throat as it apparently did in the full reverse-thrust mode.

A schematic of the flow through the engine statically and at 20 m/s in the full and partial reverse-thrust modes is presented in Fig. 15. Flow directions are based on photographs of the tufts on the external surface of the low-Mach inlet and of the line of tufts on the engine horizontal centerline 3.0 m (10 ft) in front of the inlet highlight and on the previous analysis of engine performance. The primarily axial fan jet is shown for the static and full reverse-thrust mode conditions at 20 m/s. In the partial reverse-thrust mode at 20 m/s the fan jet flow is radially outward over the inlet lip. The nacelle surface tufts in the static and partial modes were predominantly forward, while in the full reverse-thrust mode they were predominantly rearward over the nacelle surface.

The previous analysis indicates a possible explanation of the abrupt transition from the full to the partial reverse-thrust mode at a forward velocity of about 30 m/s. The primary cause of the observed reduction in reverse thrust during the transition appears to be the result of significant changes in force on the nacelle due to the increasing forward velocity. Possible flow separation from the exlet internal surface occurs, resulting in a significant decrease in the exlet's contribution to reverse thrust. Changes in surface flow on the inlet lip were observed, which would also contribute to decreased reverse thrust. It appears that the fan outlet flow is affected by the change in static pressure due to the increasing tunnel velocity, until it suddenly attaches, possibly due to the Coanda effect, to the inlet lip surface. The primarily axial fan jet then abruptly collapses and spills radially outward over the inlet lip, as indicated by the lower static pressures forward of the inlet throat. The corresponding higher inlet throat and fan-face pressures indicate a throttling effect on the fan, resulting in the observed higher fan operating line.

Some Observations of Reverse-Thrust Performance with Angle of Attack

Very limited data were obtained with angle of attack. Two cases of angle-of-attack variation on steady-state reverse thrust performance are presented in Fig. 16. Both tests were conducted at constant forward velocity with the engine initially in the partial reverse thrust mode at 0° angle of attack. In one test at 20 m/s, crosswind significantly affected reverse-thrust operation by causing the engine to abruptly change from the partial to the full reverse-thrust mode at a low angle of attack of about 3°, and then abruptly return to the partial reverse-thrust mode at about 20°. In the other test at a high forward velocity (41 m/s), no transition was observed from the partial to the full reverse-thrust mode. Crosswind also caused severe buffetting and high engine vibrations at angles of attack above 20°.

Forward-to-Reverse Thrust Transient Performance

All forward-to-reverse thrust transients were initiated from either an approach or takeoff forward-thrust engine operating condition as defined in the next section. During static (tunnel off) operation, the engine in the forward-thrust mode induced a forward velocity up to 10 m/s at the initiation of the transient. All transients had the same final reverse-blade angle of about 149° and corrected fan speed of about 85 percent.

Initial Steady-State Forward-Thrust Performance

Steady-state forward thrust performance was obtained to define the initial takeoff, aborted takeoff, and approach engine operating conditions for the forward-to-reverse thrust transient tests. Performance with the low Mach inlet is presented in Fig. 17 with both the nominal fan nozzle and the fixed reverse-thrust conical exlet. The exlet appeared to have only a very slight effect on forward thrust performance. Forward performance with the nominal fan nozzle was obtained in the NASA-Navy Lift/Cruise Inlet test program.[11,12]

The static takeoff condition was determined by operating the engine at the design fan blade angle (51.8°) and 95 percent fan speed with the tunnel off. The engine was operated at the same fan blade angle and fan speed at a forward velocity of 40 m/s for the aborted takeoff condition. A thrust level of 78 percent of the static takeoff thrust was measured at this aborted takeoff condition. The approach condition at 40 m/s was determined by operating at 95 percent of fan speed and varying fan blade angle until a thrust level equal to about 60 percent of that at the aborted takeoff condition was obtained. This condition was achieved at a fan blade angle of 44°.

Definition of Transient Terms

Terms for transient performance are shown in Fig. 18. Blade travel time (BT) is simply the time

from the demand for reverse engine thrust until the fan blade comes within 1° of the overshoot blade angle. Dwell is the time the fan blade is held at the overshoot blade angle. Flow reattachment time (RAT) is the time it takes the airflow to reverse and reattach to the fan blades after the fan blades have reached within 1° of the overshoot blade angle. Fan blade stress was used to indicate when flow reattachment occurred. As observed in previous tests, fan blade stresses increase substantially during a transient and then suddenly drop when reverse thrust was established.[6]

For the forward-to-reverse thrust transient tests, the time required to establish reverse thrust (thrust response time) is the primary parameter of interest. For these tests the thrust-response time is simply the sum of BT and RAT. An additional time period, identified in reference 6 as delay time, was not a factor in these tests and will not be discussed further. Since BT is only a function of the actuation rate and RAT is primarily an aerodynamic phenomena, transient performance will be presented here in terms of RAT and the factors that affect it.

Transient Performance with Low-Mach Inlet

Approach and takeoff forward-to-reverse thrust transient performance with the low-Mach inlet at static (tunnel off) conditions is presented in Fig. 19. Based on performance and tuft observations, all of the 20 attempted transients at static conditions were successful, with overshoot blade angles of 154° (minimum attempted) or greater. Some of these transients were initiated at forward velocities up to 10 m/s (20 knots). (These velocities were induced by forward engine operation in the wind tunnel.) As shown in the figure, increasing the overshoot blade angle results in decreasing RAT, a trend similar to that observed in previous tests with a bellmouth inlet.[6] It should be noted that increasing overshoot blade angle increases BT, but this increase is small compared with the resulting decrease in RAT. At static conditions, RAT did not appear to be significantly affected by the blade pitch-change rate. Consequently, for the approach power transients, a single curve is used to represent the range of transient performance for tunnel-off conditions. Initiating the transient from the high-power takeoff condition resulted in decreased RATs and earlier establishment of reverse thrust.

The two flagged data points indicate that for these cases RAT exceeds dwell time. This means that the flow reattached after the blade was returned from the overshoot blade angle to the final reverse blade angle. Thus, an apparent aerodynamic lag as large as 0.4 s occurred after the blade returned to the final reverse blade angle. This aerodynamic lag is also evident in the data of reference 6. A reduction in RAT may have resulted if dwell time had been increased for these cases.

Forward-to-reverse thrust transients were attempted with the low-Mach inlet at forward velocities of 20, 30, and 40 m/s (40, 60, and 80 knots). The results are presented in Fig. 20 along with the trend for the static condition for comparison. With the 20-m/s (40 knots) forward velocity, reverse thrust was established at most attempted conditions. Visual tuft observations and performance indicate that the engine, in most cases, was in a partial reverse-thrust mode after the transient. With the 40-m/s (80-knots) forward velocity, reverse thrust could not be established dynamically in four attempts (overshoot blade angles from 158° to the maximum available, 168°), and the fan remained fully stalled. Increasing the overshoot blade angle beyond the 168° actuator limit may not be effective in reducing RAT, since the blades would then be approaching the flat pitch position.

Reasonable flow reattachment times (<0.5 s) were obtained at a forward velocity of 20 m/s with an overshoot blade angle of 158.5° or greater. At an overshoot blade angle of 158° the RAT approached 1.0 s. Changing the initial forward operating condition from low power approach to high power aborted takeoff did not appreciably change the RAT. However, the aborted takeoff RATs were significantly longer at 20 m/s than those with the tunnel off.

With 30 m/s forward velocity, partial reverse thrust was established with overshoot blade angles of 166° or greater, but with longer RATs than comparable data at lower forward velocities. As noted in the figure, forward velocity requires overshoot blade angle to be increased to maintain acceptable flow reattachment times.

Transient Performance with High-Mach Inlet

All forward-to-reverse thrust transient tests with the high-Mach inlet were initiated from an approach forward-thrust engine operating condition. The results of these tests are presented in Fig. 21. At static (tunnel off) conditions reverse thrust was established at overshoot blade angles of about 164° and higher, but not at angles of 160°. Tunnel velocity was about 8 m/s at the initiation of the transient. To establish reverse thrust at tunnel-off conditions with the high-Mach inlet required significantly higher overshoot blade angles than the low-Mach inlet. This result correlates with the effect of the high-Mach inlet on the unstalling fan blade angle (discussed previously), suggesting that this inlet has a similar back pressuring effect on the stalled fan in both tests. As noted with the low-Mach inlet, RATs increased rapidly with decreasing overshoot blade angle.

At a forward velocity of 15 m/s, reverse thrust was established after both attempted transients with overshoot blade angles of about 167° (~17° of overshoot). Reattachment times were about 0.4 s. At 20 m/s reverse thrust was established three times with overshoot blade angles of about 166° and above, but in another test at 166° the engine remained in stall. Apparently, some variability exists in establishing reverse thrust after a transient, which may be associated with higher forward velocities and longer RATs. Based on the tuft observations, the engine appeared to be in a partial reverse-thrust mode after all of these transients. As was the case with the tunnel off, successful transients with the high-Mach inlet require higher overshoot blade angles than with the low-Mach inlet.

With a forward velocity of 30 m/s reverse thrust could not be established dynamically in two attempts using the full overshoot blade angle capability of 168°; the fan remained fully stalled.

Summary of Results

The reverse-thrust performance of the variable-

pitch, Q-Fan T-55 engine was obtained in the NASA Ames 40- by 80-foot wind tunnel at tunnel velocities up to 54 m/s (105 knots) and at angles of attack up to 22°.

Steady-State Reverse-Thrust Performance

1. The Q-Fan T-55 engine started at static conditions with the fan in either a stalled or unstalled mode dependent on the preset reverse-thrust fan blade angle. If initially stalled, reverse thrust was established by increasing fan speed or by increasing fan blade angle. It was more difficult to establish reverse thrust with the high-Mach inlet (smaller effective outlet throat area in reverse) than with the low-Mach inlet.

2. During the wind-tunnel tests with forward velocity, an unexpected partial reverse-thrust mode was observed with both flight-type inlets. The transition from full to partial reverse thrust occurred abruptly as the tunnel velocity was increased to about 30 m/s (60 knots) with the engine power setting held constant. The partial reverse-thrust mode was characterized by significantly lower reverse thrust, a higher fan operating line, lower inlet lip and exlet static pressures, and negligible fan jet penetration into the free stream as compared with the full reverse thrust mode. The primary cause of the observed reduction in reverse thrust in the partial mode appears to be the result of significant changes in pressure forces on the nacelle due to the increasing forward velocity. Considerable hysteresis was associated with reverting back to the full reverse thrust mode by decreasing tunnel velocity.

3. In the full reverse-thrust mode, reverse thrust increased, as expected, with increasing tunnel velocity up to about 30 m/s and the primarily axial fan jet penetrated upstream.

4. Conversely, in the partial reverse-thrust mode, increasing forward velocity from about 20 to 54 m/s (40 to 105 knots) resulted in a gradual decrease in engine reverse thrust to about 80 percent of the initial static value. The fan operating line moved significantly higher with increasing forward velocity, whereas, it moved slightly lower in the full reverse-thrust mode. The fan outlet flow remains attached to the inlet lip and spills radially outward.

5. Two steady-state reverse angle-of-attack (crosswind) tests were conducted at constant forward velocity with the engine initially in the partial reverse thrust mode at 0° angle of attack. In one test at 20 m/s, crosswind had a very significant effect on reverse operation by causing the engine to abruptly change from the partial to the full reverse-thrust mode at a low angle of attack of about 3°, and then abruptly return to the partial reverse thrust mode at about 20°. In the other test at 41 m/s no transition was observed from the partial to the full reverse thrust mode. Crosswind also caused severe buffetting and high engine vibrations at angles of attack above 20°.

Forward-to-Reverse Thrust Transient Performance

1. In the forward-to-reverse thrust transient tests, the overshoot blade angle technique proved effective in reducing the time required to establish reverse thrust with a flight-type inlet both with and without forward velocity. Forward-to-reverse transients were accomplished at up to 30 m/s forward velocity with the low-Mach inlet and up to 20 m/s with the high-Mach inlet. Above 30 m/s reverse thrust could not be established.

2. Forward velocity requires higher overshoot blade angles in order to establish and maintain reverse thrust. Increasing the overshoot blade angle results in decreasing flow reattachment times and earlier establishment of reverse thrust both statically and with forward velocity. For example, transients with the low-Mach inlet required about 2° more overshoot blade angle at 20 m/s and 9° more overshoot blade angle at 30 m/s to achieve equal flow reattachment times than those obtained statically. The high-Mach inlet requires about 6° to 10° more overshoot blade angle than the low-Mach inlet under similar operating conditions. After all successful transients, except for some conducted at 20 m/s forward velocity, the engine operated in the partial reverse thrust mode.

3. Transients performed at static conditions (tunnel off) with high-power takeoff conditions had faster reattachment times than those with low-power approach conditions, but these differences tended to disappear with forward velocity. Blade pitch change rate did not significantly affect flow reattachment time at static conditions or with forward velocity. In some transient tests the flow reattached to the fan blade after the blade was returned from the overshoot blade angle to the final reverse blade angle. This aerodynamic lag was as long as 0.4 s.

Concluding Remarks

Short-haul aircraft landing or aborted takeoff maneuvers require successful deceleration from speeds of about 40 m/s (80 knots) or higher. During aircraft deceleration thrust reversal must be initiated and maintained consistently and repeatably to prevent aircraft yawing due to dissimilar engine thrust levels. Forward velocity caused the variable pitch Q-Fan T-55 engine to operate in an unexpected partial reverse thrust steady-state mode under some operationg conditions (e.g., above 30 m/s (60 knots)). Full or partial reverse thrust was established following forward-to-reverse thrust transients only up to a forward velocity of about 30 m/s (60 knots).

However, these undesirable effects of forward velocity may be peculiar to this fan-nacelle configuration. The Q-Fan T-55 demonstrator engine had a very low (1.14) pressure ratio fan and a simple conical flared exlet. The observed characteristics may not be typical of similar higher pressure ratio fans. Furthermore, no attempt was made to modify the nacelle to reduce the adverse effects of forward velocity. Further development of advanced variable pitch turbofan engines is therefore recommended to insure adequate and reproducible reverse-thrust levels for successful aircraft deceleration.

Appendix - Symbols

BT	blade travel time, s; time from request to reverse engine thrust until fan blade reaches within 1° of overshoot blade angle
D_F	inlet diameter at diffuser exit (fan face)
D_{HL}	inlet highlight diameter
D_t	inlet throat diameter
L	inlet length from highlight to diffuser exit
M_D	aft fan duct Mach number
N	fan speed, rpm
OL	operating line
P_S	local static pressure
P_{Se}/P_{TO}	exlet wall static pressure (internal)
P_{S1}/P_{TO}	static pressure in fan inlet
P_{S2}/P_{S1}	fan static-pressure ratio (reverse)
P_T	local total pressure
P_{TO}	tunnel total pressure
P_{TI}/P_{TO}	exlet total-pressure recovery
P_{T2}/P_{TO}	fan outlet total pressure (at fan face)
P_{T2}/P_{T1}	fan pressure ratio (reverse)
$P_{T2.5}/P_{TO}$	core compressor total-pressure recovery (including exlet)
R_F	fan radius at leading edge
RAT	flow reattachment time, s; time when fan blade initially reaches within 1° of overshoot blade angle until fan comes out of stall (blade stresses drop below reference value)
RESP	thrust response time, s; time from request to reverse engine thrust until 95 percent of final reverse thrust is achieved
SLS	sea-level static
SS	steady state
TO	takeoff
T_0	ambient temperature
V_o	tunnel velocity
x	axial distance from inlet highlight
α	model angle of attack
β	fan blade angle at 3/4 radius, deg
$\Delta\beta$	relative fan blade angle, i.e., angle from design forward blade angle, deg
δ	ratio of total pressure to standard sea-level pressure
θ	ratio of total temperature to standard sea-sea-level temperature

References

1. Ciepluch, C. C., "Overview and Status of the QCSEE Program," Powered-Lift Aerodynamics and Acoustics, NASA SP-406, 1976, pp. 325-333.
2. Sagerser, D. A., Schaefer, J. W., and Dietrich, D. A., "Reverse-Thrust Technology for Variable Pitch Fan Propulsion Systems," Powered-Lift Aeronautics and Acoustics, NASA SP-406, 1976, pp. 387-402.
3. Demers, W. J., Metzger, F. B., Smith, L. W., and Wainauski, H. S., "Testing of the Hamilton Standard Q-Fan Demonstrator," Hamilton Standard, Windsor Locks, Conn., HSER-6163, Vols. 1 and 2, 1973. (NASA CR-121265.)
4. Demers, W. J., Nelson, D. J., and Wainauski, H. S., "Hamilton Standard Q-Fan Demonstrator Dynamic Pitch Change Test Program, Vol. 1," Hamilton Standard, Windsor Locks, Conn., HSER-6700-Vol.-1, 1975. (NASA CR-134861.)
5. Demers, W. J., Nelson, D. J., and Wainauski, H. S., "Hamilton Standard Q-Fan Demonstrator Dynamic Pitch Change Test Program, Vol. 2," Hamilton Standard, Windsor Locks, Conn., HSER-6700-Vol. -2, 1975. (NASA CR-134862.)
6. Schaefer, J. W., Sagerser, D. A., and Stakolich, E. G., "Dynamics of High-Bypass-Engine Thrust Reversal Using a Variable-Pitch Fan," NASA TM X-3524, 1977.
7. Giffin, R. G., McFalls, R. A., Beacher, B. F., "QCSEE Aerodynamic and Aeromechanical Performance of a 50.8 cm (20 in.) Diameter, 1.34 PR, Variable Pitch Fan with Core Flow," General Electric Co., Cincinnati, Ohio, R75AEG445, Proj. FEDD, Aug. 1977. (NASA CR-135017.)
8. Wesoky, H. L., Abbott, J. M., Albers, J. A., Dietrich, D. A., "Low-Speed Wind Tunnel Tests of a 50.8-Centimeter (20-in.) 1.15 Pressure Ratio Fan Engine Model," NASA TM X-3062, 1974.
9. Dietrich, D. A., Keith, T. G., and Kelm, G. G., "Aerodynamic Performance of Flared Fan Nozzles Used as Inlets," NASA TM X-3367, 1976.
10. Vier, W. F., "Quiet, Clean, Short-Haul Experimental Engine (QCSEE) Test Results from a 14 cm Inlet for a Variable Pitch Fan Thrust Reverser," General Electric Co., Cincinnati, Ohio, R75AEG387, Dec. 1975. (NASA CR-134867.)
11. Syberg, J., "Low Speed Test of a High-Bypass-Ratio Propulsion System with an Asymmetric Inlet Designed for Tilt-Nacelle V/STOL Airplane," Boeing Co., Seattle Wash., D-180-22888-1, Jan. 1978. (NASA CR-152072.)
12. Shain, W. M., "Test Data Report, Low-Speed Wind Tunnel Tests of a Full-Scale Lift/Cruise-Fan Inlet, with Engine, at High Angles of Attack," Boeing Commercial Airplane Co., Seattle, Wash., T6-6145, Jan. 1978. (NASA CR-152055.)

Table 1 Q-Fan T-55 Engine-inlet comparison

	Asymmetric, low-Mach inlet	High Mach inlet
Fan hub-tip ratio	0.46	0.46
D_F, cm (in.)	139.7 (55)	139.7 (55)
D_t/D_F	0.855 av.	0.80
A_t/A_F	0.932	0.809
$(D_{HL}/D_t)^2$	1.30 - 1.76	1.46
D_t, cm (in.)	120.0 (47.2) av.	111.8 (44)
D_{HL}, cm (in.)	146.9 (57.8) av.	135.1 (53.2)
Equivalent diffuser angle	6.1°	6.9°
L/D_F	0.82	1.01
Lip contour (internal)		2:1 ellipse

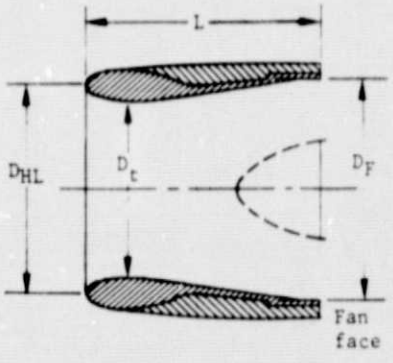

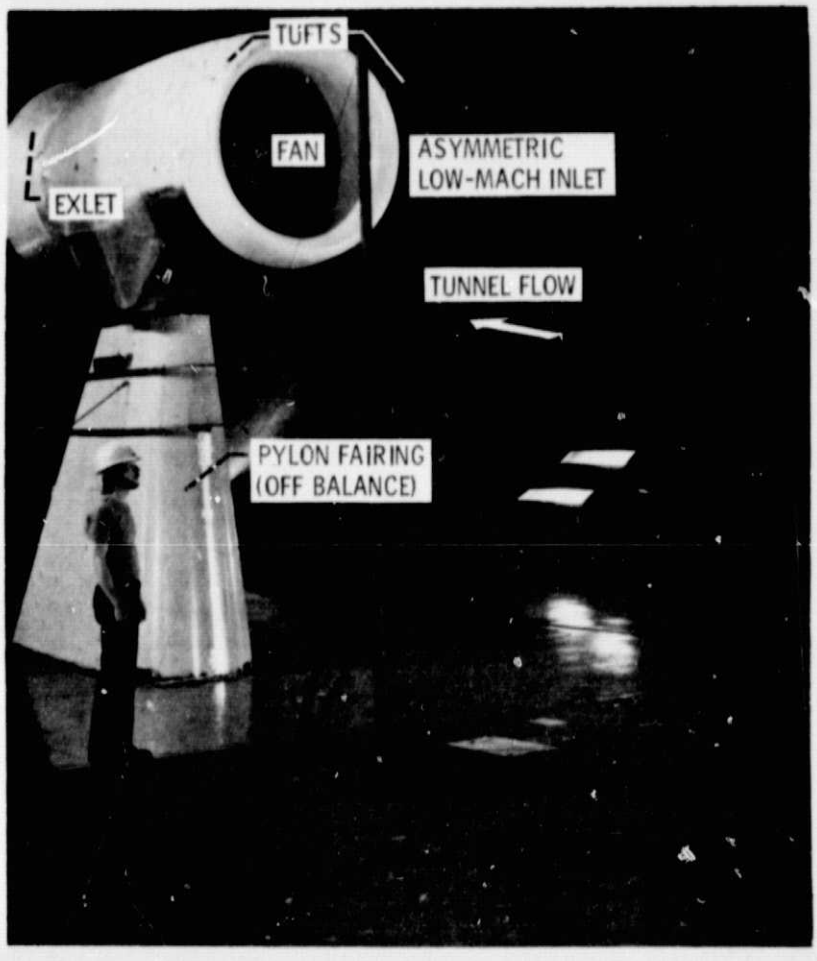

Figure 1. - Q-fan T-55 engine installed in Ames 40- by 80-ft wind tunnel.

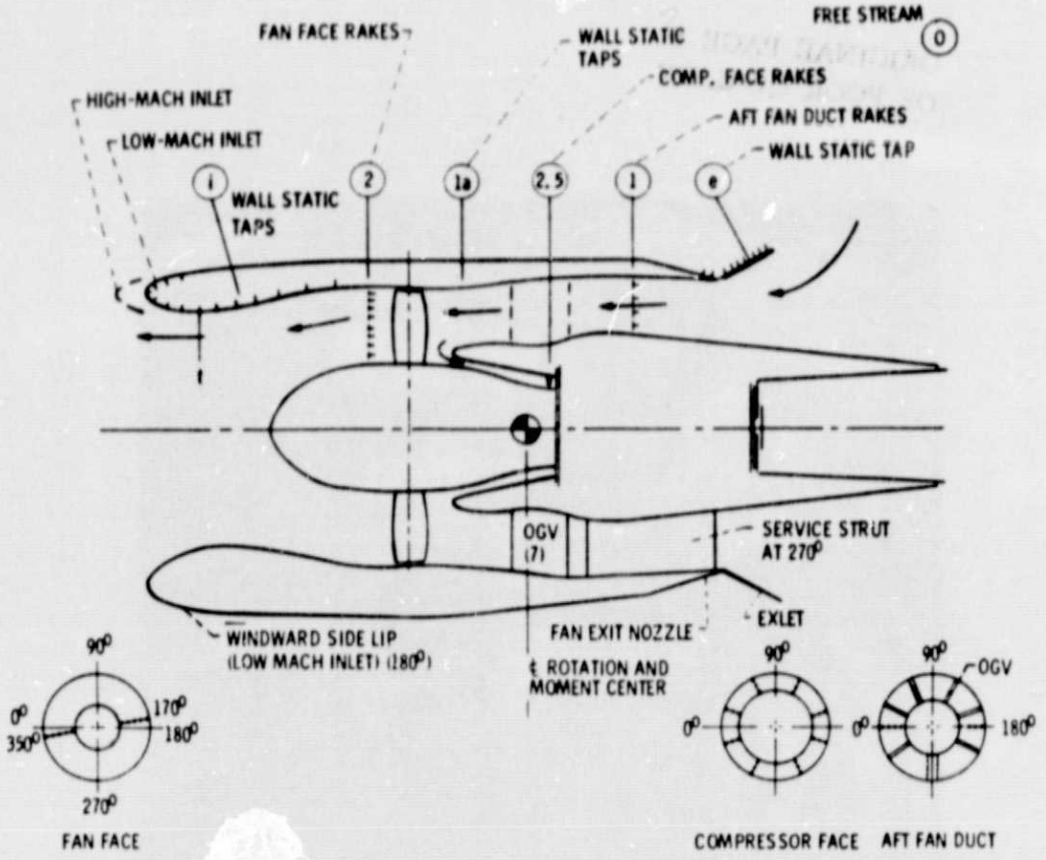

Fig. 2 Q-fan T-55 engine reverse-thrust configuration.

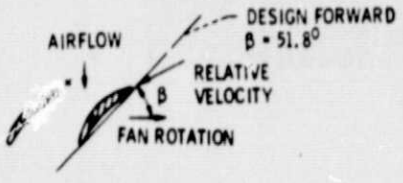

(a) Forward thrust.

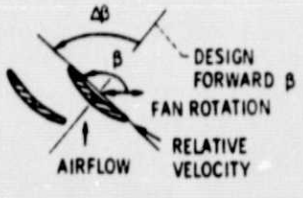

(b) Reverse thrust through feather (stall) pitch.

Fig. 3 Fan blade angle convention.

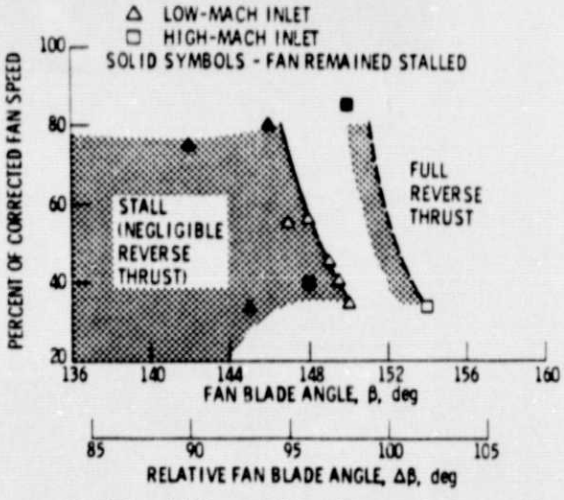

Fig. 4 Fan stall-to-unstall transition speed. (Fan speed increased at constant β at startup.) Static conditions.

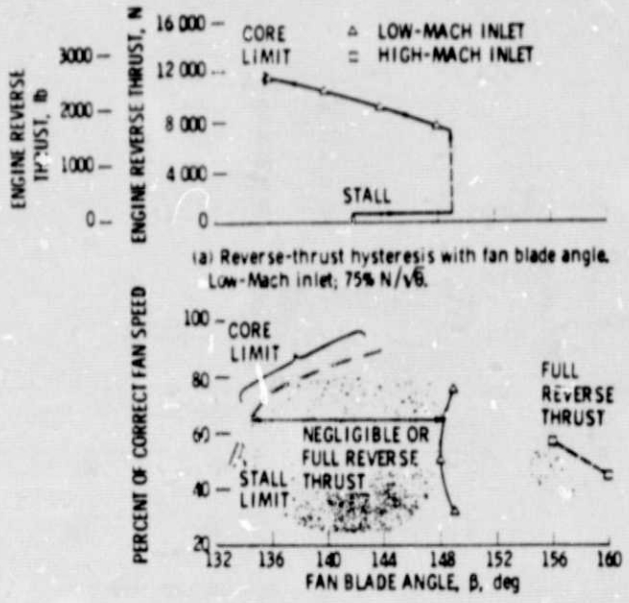

(a) Reverse-thrust hysteresis with fan blade angle. Low-Mach inlet; 75% $N/\sqrt{\theta}$.

(b) Effect of slow β variation on steady-state reverse-thrust operating range.

Fig. 5 Effect of fan blade angle on steady-state reverse thrust at static conditions.

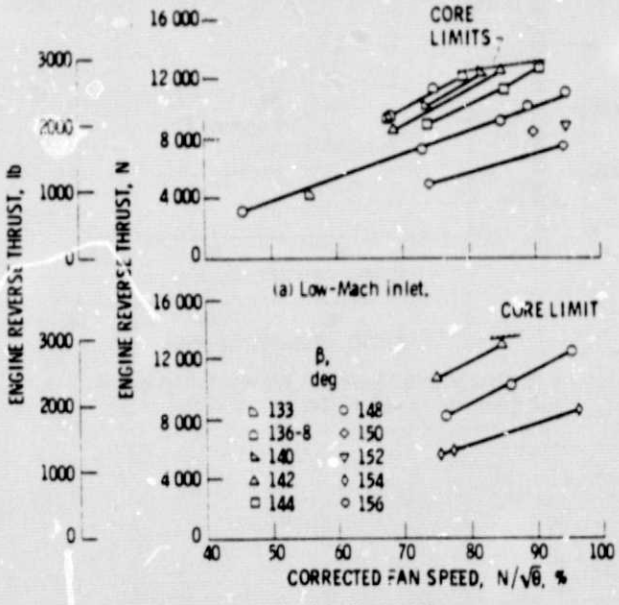

(a) Low-Mach inlet.

(b) High-Mach inlet.

Fig. 6 Q-fan T-55 engine steady-state reverse-thrust performance. Static conditions.

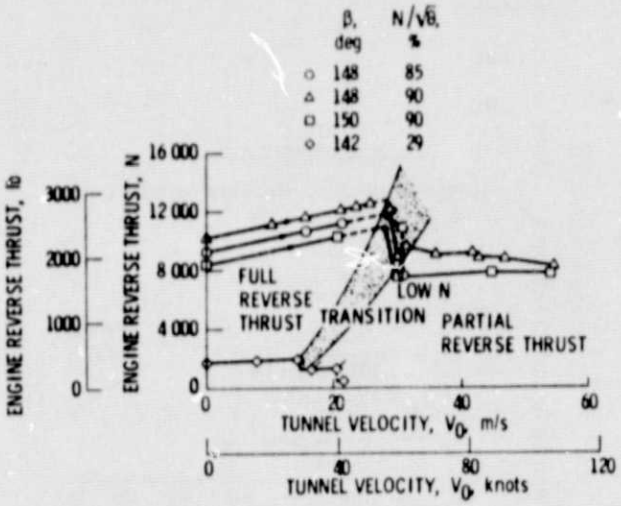

Fig. 7 Effect of increasing tunnel velocity on steady-state reverse-thrust performance. Low-Mach inlet; $\alpha = 0^0$.

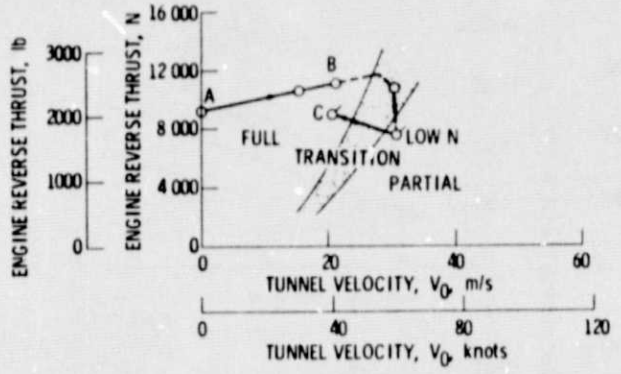

Fig. 8 Reverse-thrust hysteresis loop with tunnel velocity. Low-Mach inlet, $\alpha = 0^0$; $\beta = 148^0$; $N/\sqrt{\theta} \sim 85\%$.

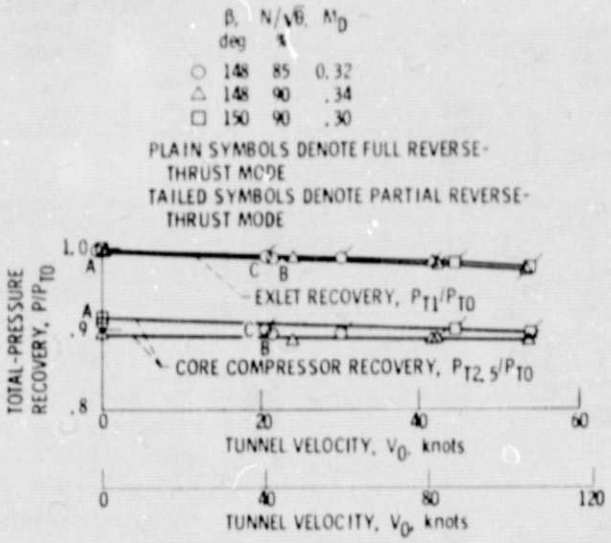

Fig. 9 Effect of tunnel velocity on exlet and core compressor total-pressure recovery. Low-Mach inlet, $\alpha = 0^0$.

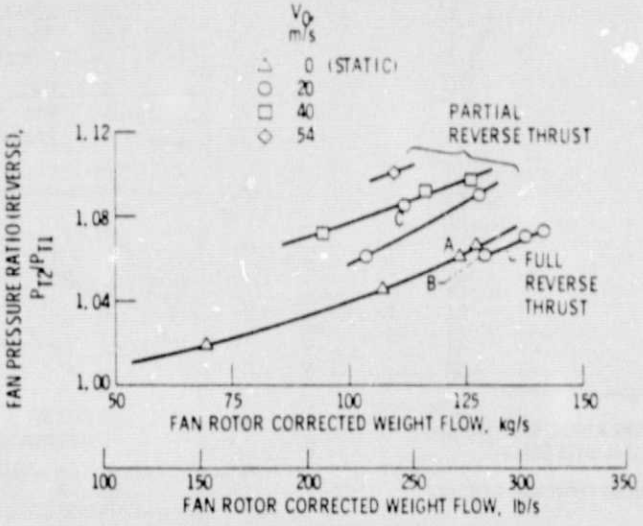

Fig. 10 Steady-state reverse-thrust fan performance at several forward velocities. Low-Mach inlet, $\alpha = 0^0$; $\beta = 148^0$.

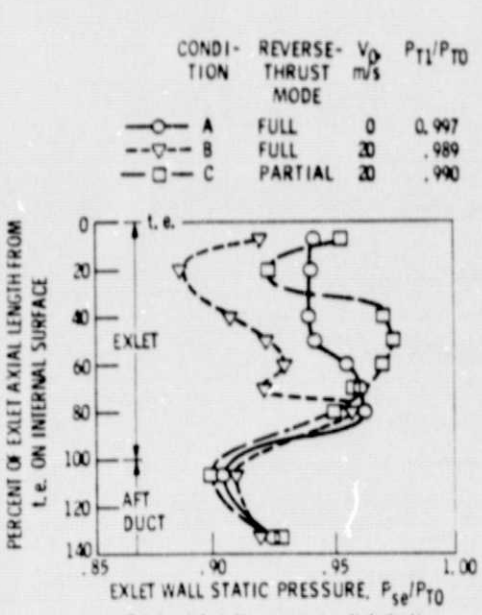

(a) Exlet axial static-pressure distribution, windward side.

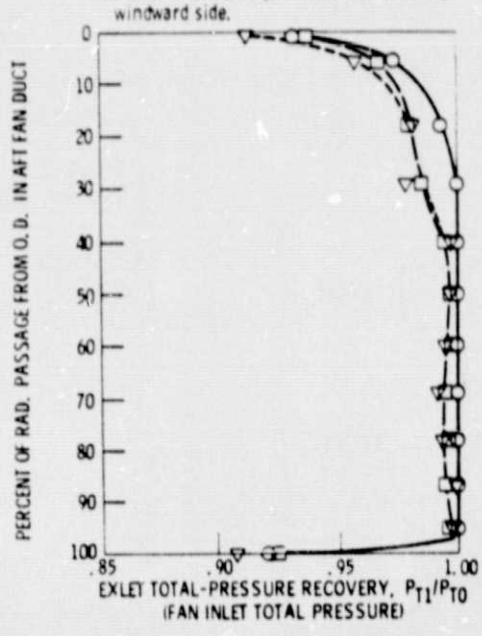

(b) Aft fan duct (fan inlet) radial total-pressure distribution.

Fig. 11 Exlet and aft fan duct pressure profiles $\beta = 148^0$; $N/\sqrt{\theta} \sim 85\%$; $A_{te}/A_D = 2.0$; $M_D \sim 0.30$ to 0.35.

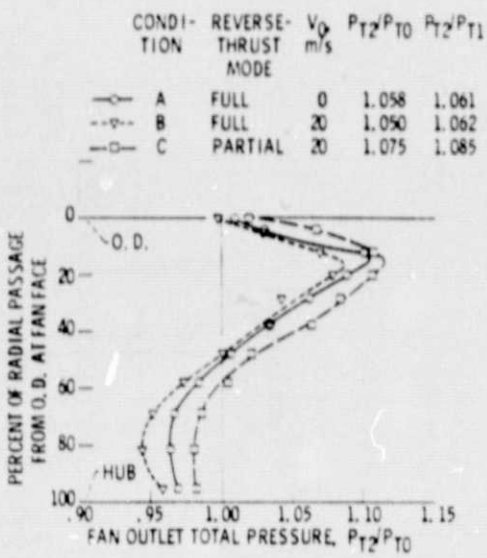

Fig. 12 Fan outlet radial pressure distribution in full and partial reverse-thrust modes. Low-Mach inlet; $A_t/A_F = 0.932$; $\beta = 148^0$; $N/\sqrt{\theta} \sim 85\%$.

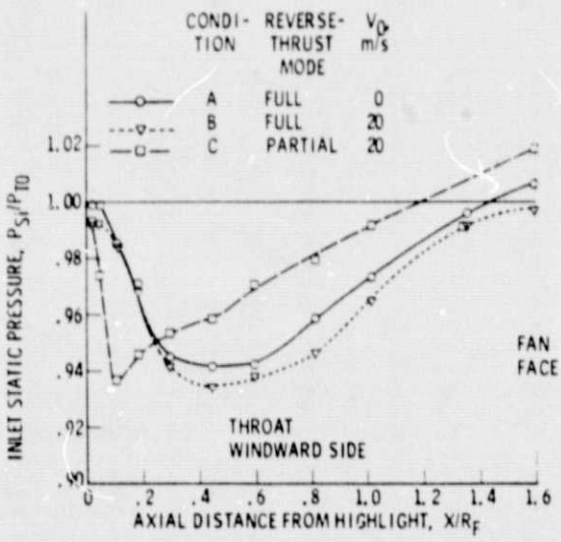

Fig. 13 Inlet axial static-pressure profiles. Low-Mach inlet, windward side; $\beta = 148^0$; $N/\sqrt{\theta} \sim 85\%$. Tunnel $P_S/P_{T0} = 0.997$ AT 20 m/s.

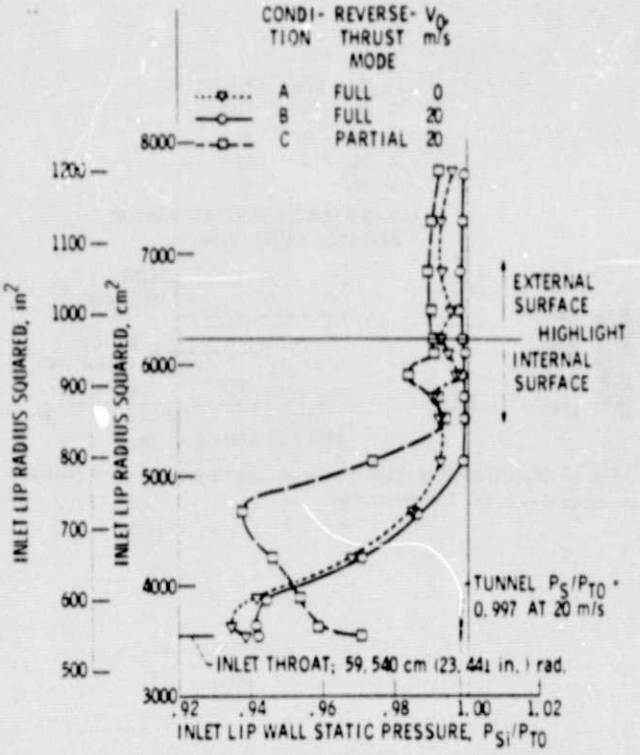

Fig. 14 Inlet lip wall static-pressure radial profile. Windward side; $\beta = 148^0$; $N/\sqrt{\theta} \approx 85\%$.

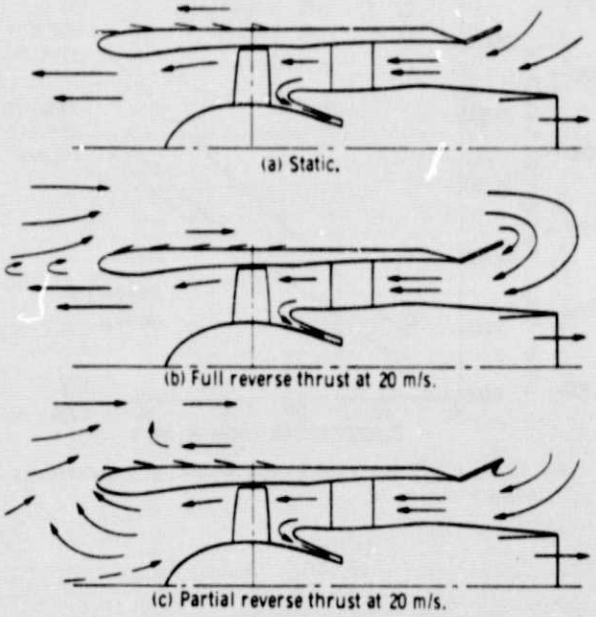

(a) Static.

(b) Full reverse thrust at 20 m/s.

(c) Partial reverse thrust at 20 m/s.

Fig. 15 Reverse-thrust flow patterns. $\beta = 148^0$; $N/\sqrt{\theta} = 85\%$.

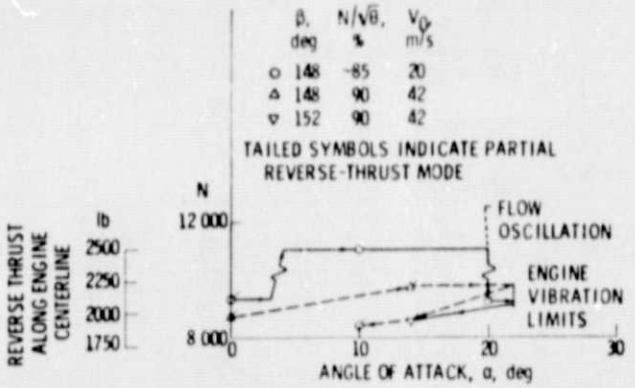

Fig. 16 Effect of angle of attack on steady-state reverse thrust at constant forward velocity. Low-Mach inlet.

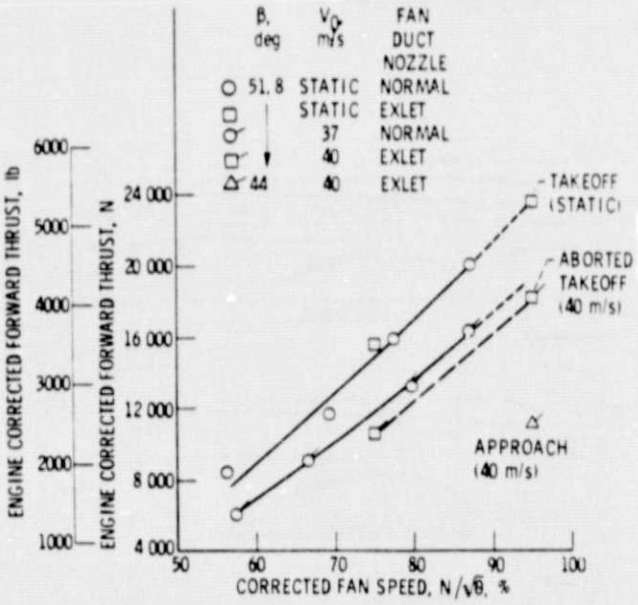

Fig. 17 Q-fan T-55 engine steady-state forward thrust performance. Low-Mach inlet; $\alpha = 0^{0}$.